学位論文（博士）

Doctoral Thesis

**Experience-specific plasticity at excitatory and inhibitory synapses
onto granule cells in the dentate gyrus**

（ 海馬歯状回の顆粒細胞における経験特異的なシナプス可塑性)

Name（氏名）　　　 : Han Thiri Zin（ハン ティリ ジン）

Affiliation（所属）: Yamaguchi University Graduate School of Medicine
（山口大学大学院医学系研究科）

Major（専攻）　　 : Medicine（医学専攻）

Course（講座）　　 : Physiology（神経生理学講座）

Contents

Abstract

The hippocampal dentate gyrus has been identified to play a critical role in maintaining contextual memory in many mammalian species. To evaluate learning-induced synaptic plasticity of granule cells, we subjected male rats to an inhibitory avoidance (IA) task and prepared acute hippocampal slices. In the presence of 0.5 µM tetrodotoxin, we recorded miniature EPSCs and IPSCs in male rats experiencing four groups: untrained, IA-trained, unpaired, and walk-through. Compared with the untrained, IA-trained, unpaired, and walk-through groups, the unpaired group significantly enhanced mean mEPSC amplitudes, suggesting the experience-induced plasticity at AMPA receptor-mediated excitatory synapses. For inhibitory synapses, both unpaired and walk-through groups significantly decreased mean mIPSC amplitudes, showing the experience-induced reduction of postsynaptic GABA$_A$ receptor-mediated currents. Unlike the plasticity at CA1 synapses, it was difficult to explain the learning-specific plasticity at the synapses. However, overall multivariate analysis using four variables of mE(I)PSC responses revealed experience-specific changes in the diversity, suggesting that the diversity of excitatory/inhibitory synapses onto granule cells differs among the past experience of animals include the learning.

In comparison with CA1 pyramidal neurons, granule cells consistently showed greater amplitude and frequency of mE(I)PSCs. Fluctuation analysis further revealed that granule cells provide more postsynaptic AMPA receptor channels and greater single-channel current of GABA$_A$ receptors of than CA1 pyramidal neurons. These findings show functional differences between two types of principal cells in the hippocampus.

Introduction

The first evidence of a Hebb-like synaptic plasticity event was discovered in the dentate gyrus (DG) of a rabbit hippocampus (Bliss and Lømo, 1973). Brief tetanic stimulation of the perforant path has persistently strengthened the stimulatory response in the DG, and the long-term potentiation (LTP) came to be viewed as a synaptic model of learning and memory.

Both AMPA- and NMDA-type glutamate receptors mediate perforant path stimulation at the synapses on granule cells (Bliss and Collingridge, 1993). The LTP not only enhances the presynaptic release of glutamate (Dolphin et al., 1982) but also increases ^{3}H-AMPA receptor binding in the DG and CA1 (Tocco et al., 1992). NMDA receptors are known to play a significant role in LTP induction, as proved by results showing that a specific antagonist of this receptor can block LTP induction without affecting AMPA receptor-mediated synaptic transmission (Collingridge et al., 1983). More importantly, bilateral blockade of LTP in the DG synapses also impairs hippocampal-dependent learning (Morris et al., 1986), suggesting a role for LTP in learning. Although granule cells in the DG are considered essential to learning function by decorrelating overlapping input patterns *in vivo* (GoodSmith et al., 2017), conclusive evidence for learning and induced synaptic plasticity in these cells remains to be lacking (Neuneubel and Knierim 2014).

To evaluate the plasticity, we previously showed contextual learning-dependent plasticity in CA1 pyramidal neurons. Contextual learning strengthened excitatory synapses through the synaptic incorporation of AMPA-type glutamate receptors. It also strengthened GABA$_A$ receptor-mediated inhibitory synapses on hippocampal pyramidal CA1 neurons, thus generating a broad diversity of excitatory/inhibitory synaptic inputs in individual CA1 neurons (Mitsushima et al., 2013; Sakimoto et al., 2019). Using the

2

same experimental protocol, we evaluated the synaptic plasticity of granule cells in the untrained, IA-trained, unpaired, and walk-through animals to examine the learning-specific change.

Results

IA task

To investigate learning-induced plasticity at DG synapses in granule cells, we subjected rats to an IA task (Fig. 1A; Izquierdo et al., 1998; Mitsushima et al., 2011, 2013). In this learning paradigm, rats could cross from a light box to a dark box, where an electric foot-shock (1.6 mA, 2 s) was delivered. Half an hour after the IA task, we measured the latency in the illuminated box as representing contextual learning performance. The latency was much longer after training than before training (Fig. 1B; $t_9 = 27.607$; $P < 0.0001$) with paired foot-shock.

Miniature of postsynaptic currents and frequencies events in granule cells

To analyze experience-induced synaptic plasticity, we recorded mEPSCs at −60 mV and mIPSCs at 0 mV sequentially in the same neuron in the presence of tetrodotoxin (0.5 μM) on both sides of the dorsal hippocampus (Fig. 2A). By changing the membrane potential, we sequentially recorded mEPSCs (at −60 mV) and mIPSCs (at 0 mV) from the same neuron, as has been reported previously (Mitsushima et al., 2013). The postsynaptic currents correspond to the response elicited by a single vesicle of glutamate or GABA. In contrast, the number of synapses affects event frequency (Pinheiro and Mulle, 2008).

At the synapses in granule cells, we measured each neuron's strength of AMPA receptor-mediated excitatory inputs versus $GABA_A$ receptor-mediated inhibitory inputs.

We then prepared acute brain slices 30 minutes after the animals completed the behavioral paradigm and recorded the mEPSCs at 60 mV in the neurons. We detected an overall difference in mEPSC amplitude among untrained, IA-trained, unpaired, and walk-through animals (Fig. 2D, $F_{3,125} = 4.431$, $P = 0.0054$). *Post-hoc* analysis showed that the experience of task significantly increased mEPSC amplitudes in the unpaired ($P = 0.00079$), but not in the trained or walk-through groups. Similarly, in mIPSC amplitude, we found an overall difference (Fig. 2D, $F_{3,125} = 6.516$, $P = 0.0004$). *Post-hoc* analysis showed that the experience significantly decreased mIPSC amplitudes in the unpaired ($P = 0.002$) or walk-through ($P = 0.001$) but not in the trained groups. Conversely, in mEPSC frequency, there is no overall significance among the four groups (Fig. 2E, $F_{3,125} = 0.168$, $P = 0.92$). In mIPSC frequency, we found an overall difference (Fig. 2E, $F_{3,125} = 6.521$, $P = 0.0004$), and *post-hoc* analysis showed that the experience significantly increased in the unpaired ($P = 0.0003$) or walk-through ($P = 0.0003$) groups.

To evaluate the experience specificity, we plotted the four parameters in a four-dimensional virtual space in order to analyze both amplitude and frequency of mEPSC and mIPSC events in individual granule cells. We used one-way multivariate ANOVA (MANOVA) with experience as the between-group factor, which showed a significant main effect of experience (Figs. 2B and C; $F_{12, 323} = 4.680$, $P < 0.0001$). *Post-hoc* MANOVA further showed differences between two specific experiences (Table 1), suggesting experience-specific synaptic plasticity of the DG granule cells.

Specific plasticity at perforant pathway or Mossy cell synapses in granule cells

To further examine specific changes at medial perforant pathway (MPP), lateral perforant pathway (LPP), or Mossy cell synapses, we recorded evoked EPSCs of

granule cells in untrained or IA trained rats (Fig. 3). To determine the extent of pathway-specific postsynaptic plasticity, we measured currents mediated by AMPA receptors and NMDA receptors at these synapses. Although no significant change was observed at specific synapses, IA training significantly increased the AMPA/NMDA ratio by the combination of MPP and LPP data ($U = 623$, $P = 0.03$, Fig 3A left and middle panels). These results suggest that the training postsynaptically strengthened perforant path synapses in granule cells.

Moreover, we investigated presynaptic change at MPP, LPP and mossy cells synapses after the training. As shown in Fig. 3B, we applied paired stimuli at 100-ms intervals, recorded paired-pulse responses, and calculated the PPRs to determine glutamate release probability at the excitatory synapses. we recorded at MPP, LPP and mossy cells synapses of granule cells. Although no significant presynaptic change was observed at MPP and LPP synapses, IA training significantly increased in the PPRs at mossy cells synapses ($U = 245$, $P = 0.03$, Fig. 3B right). This result suggests that the training induced presynaptic plasticity by reducing the glutamate release probability at mossy cell synapses.

Table 1 *Post-hoc* MANOVAs for Figure 2

Group	Untrained	IA-trained	Unpaired	Walk-through
Untrained	–	$F_{4,62} = 2.900$	$F_{4,62} = 9.566$	$F_{4,64} = 6.933$
IA-trained	$P = 0.0289$	–	$F_{4,55} = 4.166$	$F_{4,57} = 3.437$
Unpaired	$P < 0.0001$	$P = 0.0051$	–	$F_{4,57} = 2.007$
Walk-through	$P = 0.0001$	$P = 0.0138$	$P = 0.1057$	

Comparison with CA1 pyramidal neurons

By comparing mE(I)PSC data in CA1 pyramidal neurons (Sakimoto et al., 2019), we found further cell-specific differences in untrained conditions (Table 2). At excitatory synapses, granule cells showed greater mEPSC amplitudes/frequency than CA1 pyramidal neurons. Further fluctuation analysis indicated greater number of postsynaptic open Na^+ channels without changing single channel currents of granule cells.

Also, at inhibitory synapses, granule cells were noted to exhibit greater mIPSC amplitudes/frequency than CA1 pyramidal neurons. Further fluctuation analysis indicated greater single Cl^- channel currents without changing the number of open channels of granule cells conditions (Table 2). At excitatory synapses, granule cells showed greater mEPSC amplitudes/frequency than CA1 pyramidal neurons. Further fluctuation analysis indicated greater number of postsynaptic open Na^+ channels without changing single channel currents of granule cells.

Also, at inhibitory synapses, granule cells were noted to exhibit greater mIPSC amplitudes/frequency than CA1 pyramidal neurons. Further fluctuation analysis indicated greater single Cl^- channel currents without changing the number of open channels of granule cells.

Table 2   A comparison of granule cells and CA1 pyramidal neurons

---

Parameters	Granule cells	CA1 neurons	*P*-value
mEPSC amplitudes pA	15.4 ± 0.5 (37)	12.8 ± 0.3 (56)	< 0.0001
mEPSC frequency per 5 min	28.0 ± 4.0 (37)	7.6 ± 0.9 (56)	< 0.0001
number of open Na^+ channels	32.6 ± 7.8 (16)	15.2 ± 2.1 (42)	= 0.046
single Na^+ channel currents pA	2.0 ± 0.4 (16)	2.9 ± 0.6 (42)	ns
mIPSC amplitudes pA	23.5 ± 1.1 (37)	16.3 ± 0.5 (56)	< 0.0001
mIPSC frequency per 5 min	43.7 ± 3.9 (37)	68.7 ± 5.8 (56)	< 0.0001
number of open Cl^- channels	28.0 ± 11.5 (23)	31.3 ± 3.6 (23)	ns
single Cl^- channel currents pA	6.2 ± 1.4 (23)	1.6 ± 0.5 (23)	= 0.004

Parentheses indicate the number of cells.

Discussion

A single granule cell is known to receives inputs of approximately 5600 excitatory (Patton and McNaughton, 1995, Amaral et al., 2007) and 950 inhibitory synapses (Halasy and Somogyi, 1993). Although we detected variable experience-induced plasticity at excitatory or inhibitory synapses, it was difficult to clarify the learning-specific change at the synapses. If it is experience with IA apparatus, 3 experience groups (trained, unpaired, walk-through) should be different from the untrained group but be similar to each other. Alternatively, the experience could be "time spent in the dark box," where groups that spend more time on the dark box may

promote plastic change at GABAergic inhibitory synapses. To extract context-specific or learning-dependent plasticity, input-specific and/or cell-specific analysis of the plasticity should be necessary in granule cells.

Granule cells received three types of glutamatergic inputs. The layer II neurons of the entorhinal cortex projected to the cells *via* lateral and medial perforant paths (Patten et al., 2015), and mossy cells in the *hilus* also projected to the cells (Hashimotodani et al., 2017, Bui et al., 2018). Medial entorhinal area cells are known to contain several spatially modulated cell types, such as border cells, head cells, direction cells, victor cells, and grid cells. In contrast, lateral entorhinal area cells preferentially represent non-spatial information, such as objects and object-related spatial features, including egocentric bearing toward an object or previous object locations (Hainmueller and Bartos, 2020). Optogenetic induction of LTP at perforant path synapses of engram cells in the DG restored spine density and fear-conditioned memory, suggesting a role for performant path synapses in memory (Roy et al., 2016). Moreover, glutamatergic inputs from the mossy cells may be essential for learning because optogenetic inhibition of hilar mossy cell activity impedes the encoding of spatial context (Bui et al., 2018).

Since the synaptic plasticity was learning-dependent in CA1 pyramidal neurons, we further compared the miniature currents between the two principal cell types (Table 2). Considering the results of fluctuation analysis, more postsynaptic AMPA receptor channels may contribute to form greater mEPSC amplitudes than CA1 pyramidal neurons. In contrast, at inhibitory synapses, greater single-channel current of $GABA_A$ receptors may form greater mIPSC amplitudes than CA1 pyramidal neurons. Because the expression of individual $GABA_A$ receptor subunits in DG was different from that in CA1 (Palpagama et al., 2019), the composition of $GABA_A$ receptor subunits in DG may contribute to increase the single-channel current.

Regarding the number of synapses, the neuro-anatomical analysis estimated that single suprapyramidal granule cells (approximately 5600: Amaral et al., 2007) have smaller excitatory synapses than single CA1 pyramidal neuron (about 13,000 to 30,000: Bezaire and Soltesz, 2013). In these present results, however, granule cells showed much higher mEPSC frequency than CA1 pyramidal neurons. Since the mE(I)PSC frequency seems to represent the number of functional synapses or the presynaptic release probability (Pinheiro and Mulle, 2008), a great population of silent synapses in CA1 pyramidal neurons (Shi et al., 2001) may cause the low mEPSC frequency in CA1 neurons. Also, the high presynaptic glutamate release probability onto granule cells (Dolphin et al., 1982) may contribute to elevate mEPSC frequency in granule cells. Consequently, the difference may contribute to forming the typical firing pattern in DG granule cells. Spontaneous firing rates of granule cells were extremely low when rats were awaken (Jung and McNaughton, 1993; Senzai and Buzsaki 2017; GoodSmith et al., 2017), which is quite different from the firings of CA1 pyramidal neurons (Danjo et al., 2018; Ishikawa et al., 2019).

We further analyzed how the perforant pathway or the mossy cells in dentate gyrus deal with contextual learning. The medial perforant pathway (MPP) originates from the medial entorhinal cortex and terminates in the middle one third of the dentate gyrus molecular layer, whereas the lateral perforant pathway (LPP) originates from lateral entorhinal cortex and terminates on outer one third of the dentate molecular layer. The MPP and LPP inputs to the hippocampal dentate gyrus form two distinct laminar inputs onto the middle and distal aspects of the granule cell dendrites (Wang, 1997). The training significantly increased AMPA/NMDA ratio at the synapses, suggesting training-induced postsynaptic plasticity at perforant pathway synapses in granule cells.

Mossy cells also comprise a large fraction in the hippocampus dentate gyrus region. Their function is important because they are vulnerable to some pathological conditions like ischaemia, traumatic brain injury and seizures (Helen E. Schafman, 2016). Loss of the cells can contribute to the dysfunction of dentate gyrus, suggesting critical role for the hippocampal memory (Helen E. Schafman, 2016). The vulnerability of mossy cells may arise as a result of a strong input that they receive from granule cells, their pattern of gene expression, subcellular metabolism and physiological properties (Helen E. Schafman, 2016). The training significantly increased paired pulse ratio at the Mossy cell–granule cell synapses, suggesting training-induced decrease in presynaptic glutamate release probability at Mossy cell synapses in granule cells.

Conclusion

We sequentially recorded mEPSCs and mIPSCs from the same granule cells to obtain four variables (mEPSC/mIPSC amplitudes and frequency). Unlike the plasticity at CA1 synapses, it was difficult to identify learning-specific plasticity in granule cells. However, we detected variable experience-induced plasticity at excitatory or inhibitory synapses. Moreover, overall MANOVA with four variables revealed experience-specific plasticity at excitatory/inhibitory synapses, suggesting that the diversity of excitatory/inhibitory synapses differs among the past experience of animals.

In comparison with CA1 pyramidal neurons, granule cells exhibited greater mE(I)PSC responses, providing more postsynaptic AMPA receptor channels and greater single-channel current of $GABA_A$ receptors than CA1 pyramidal neurons. These findings show functional differences between the two principal cell types in the dorsal hippocampus.

Experimental procedure

Animals

Male Sprague Dawley rats (postnatal 4 weeks of age) were obtained from Chiyoda Kaihatsu Co., Tokyo, Japan. Prior to the experiment, the rats were individually housed in plastic cages for a couple of days (40 cm × 25 cm × 25 cm) at a constant temperature of 23 °C ± 1 °C under a constant cycle of light and dark (lights on: 8:00 AM to 8:00 PM) with ad libitum access to water and food (MF, Oriental Yeast Co. Ltd, Tokyo Japan). All animal housing and surgical procedures followed the guidelines of the Institutional Animal Care and Use Committee of Yamaguchi University. These guidelines comply with the Guide for the Care and Use of Laboratory Animals published by the National Institute of Health (NIH Publication No. 85-23, revised 1996).

Inhibitory avoidance (IA) task

Hippocampus-dependent IA training procedures were described previously (Mitsushima et al., 2011, 2013). The IA training apparatus (length: 33 cm; width: 58 cm; height: 33 cm) was a two-chambered box consisting of a lit safe side and a dark shock side separated by a trap door (Fig. 1A). For training, rats were placed in the lit side of the box, facing the corner opposite the door. After the trap door was opened, the rats could enter the dark box at will. The latency before entering the novel dark box was measured as a behavioral parameter (latency before IA learning, Fig 1B). Soon after the animals entered the dark side, we closed the door and applied a scrambled electrical foot shock (1.6 mA, 2 s) via electrified steel rods placed in the floor of the box. The rats were kept in the dark compartment for 10 s before being returned to their home cage. Untrained control rats were not moved from their home cages, and injected with the

same dose of anesthesia. The unpaired control rats (foot shock only) were housed in the shock cage and subjected to the same scrambled electrical foot shock without any contextual experience. The walk-through control rats were placed in the IA training apparatus and allowed to explore for 1 min, without shock (IA trained group: n = 10; walk-through group: n = 8; unpaired group: n = 7; untrained group: n = 10).

Thirty minutes after the procedure described above, the rats were placed in the lit side of the box. The latency before entering the dark box was measured as an indicator of learning performance (latency after IA learning).

Electrophysiological recordings

One hour after the paired foot-shock, rats were anesthetized with pentobarbital and acute brain slices prepared (Mitsushima et al., 2011, 2013). Preparation of brain slices using the mixture of ketamine (75-100 mg/kg sc) and xylazine (10 mg/kg sc) anesthesia did not affect the mE(I)PSC amplitude and frequency.

For the whole-cell recordings (Kida et al., 2016, 2017), the brains were quickly perfused with ice-cold dissection buffer (25.0 mM $NaHCO_3$, 1.25 mM NaH_2PO_4, 2.5 mM KCl, 0.5 mM $CaCl_2$, 7.0 mM $MgCl_2$, 25.0 mM glucose, 90 mM choline chloride, 11.6 mM ascorbic acid, 3.1 mM pyruvic acid) and gassed with 5% CO_2/95% O_2. Coronal brain slices (target CA1 area: AP -3.8 mm, DV 2.5 mm, LM ± 2.0 mm) were cut (350 μm, Leica vibratome, VT-1200) in dissection buffer and transferred to physiological solution (22–25°C, 114.6 mM NaCl, 2.5 mM KCl, 26 mM $NaHCO_3$, 1 mM NaH_2PO_4, 10 mM glucose, 4 mM $MgCl_2$, 4 mM $CaCl_2$, pH 7.4) gassed with 5% CO_2/95% O_2). The recording chamber was perfused with physiological solution at 22-25°C. For the mEPSC and mIPSC recordings, we used the physiological solution containing 0.5 μM TTX to block Na^+ channels.

Patch recording pipettes (4–7 MΩ) were filled with intracellular solution (127.5 mM cesium methanesulfonate, 7.5 mM CsCl, 10 mM Hepes, 2.5 mM $MgCl_2$, 4 mM Na_2ATP, 0.4 mM Na_3GTP, 10 mM sodium phosphocreatine, 0.6 mM EGTA at pH 7.25). Under the IR-DIC microscope (BX50, Olympus, Tokyo, Japan), recording cells were randomly selected in the upper blade of the DG (Fig. 1C). Whole-cell recordings were obtained from the cells using an Axopatch-1D amplifier (Axon Instruments Inc., Union City, CA, USA). The whole-cell patch-clamp data were collected using a Clampex 10.4 instrument, and the data were analyzed using Clampfit 10.4 software (Axon Instruments).

For the miniature recordings, the mEPSCs (-60 mV holding potential) and mIPSCs (0 mV holding potential) were recorded sequentially for 5 min in the same neuron. The miniature events were detected using the Clampfit 10.4 software (Axon Instruments), and the events above 10 pA were used in the analysis. We recorded for at least 5 min, to determine the event frequency of mEPSCs or mIPSCs. The amplitudes of the events were averaged to obtain the mean amplitude. Bath application of an AMPA receptor blocker (CNQX, 10 μM) or $GABA_A$ receptor blocker (bicuculline methiodide, 10 μM) consistently blocked the mEPSC or mIPSC events, respectively. Although CNQX is a competitive antagonist of AMPA receptor and glycine site of NMDA receptors, extracellular Mg^{2+} is known to block NMDA receptors when the resting potential is less than -40 mV in CA1 pyramidal neurons (Otmakhova et al., 2002).

To analyze the function of MPP and LPP synapses, a bipolar tungsten stimulating electrode (Unique Medical Co., Ltd., Tokyo, Japan) was placed in the molecular layer of dentate gyrus, at ~200–300 mm dorsal to the recorded cell body for LPP. For MPP, the stimulating electrode was placed in the molecular layer of dentate gyrus, at ~50–200 mm dorsal to the recorded cell body. To analyze the function of mossy cells synapses,

the stimulating electrode was placed in the hilar region of dentate gyrus. For postsynaptic plasticity, we measured the ratio of AMPA receptor-mediated postsynaptic current to NMDA receptor-mediated current (AMPA/NMDA). This ratio was calculated as the ratio of the peak current at -60 mV to the current at +40 mV, at 150 ms after stimulus onset (40–60 traces were averaged for each holding potential). For presynaptic plasticity, 50–100 sweeps were recorded with paired stimuli applied at 100-ms intervals with 0.4 Hz frequency (1 trace per 2.5 sec), and the ratio of the second amplitude to the first amplitude was calculated as the PPR.

Nonstationary fluctuation analysis

AMPA receptor-mediated mEPSCs and GABA$_A$ receptor-mediated mIPSCs were analyzed by nonstationary fluctuation analysis (Ono et al. 2016, Sakimoto et al., 2019). To isolate fluctuations in current decay due to stochastic channel gating, the mean waveform was scaled to the peak of individual E(I)PSCs. The requirements for such analysis include a stable current decay time course throughout the recording and an absence of any correlation between the decay time course and peak amplitude. The relationship between the peak-scaled variance and the mean current is given by the following equation:

$$\sigma^2 = iI - I^2/N + b_l$$

where σ^2 is the variance, I is the mean current, N is the number of channels activated at the peak of the mean current, i is the unitary conductance, and bl is the background variance. In our experiments, 31–69 EPSCs and 14–133 IPSCs were analyzed from selected epochs in each of the cells in which there was no correlation between current decay (63% decay time) and peak amplitude ($P > 0.05$, Spearman's rank-order correlation test). The weighted mean channel current can be estimated by fitting the full

parabola or initial slope of the relationship. All the analysis was done using MATLAB

software (MathWorks, MA, USA).

Statistical analysis

      We used the paired *t*-test to analyze IA latency, and unpaired *t*-test to compare the

miniature data between granule cells and CA1 pyramidal neurons. One of the four

miniature parameters (i.e. mEPSC amplitudes) was analyzed by one-way factorial

analysis of variance (ANOVA) where the variable was the experience. The ANOVA was

followed by *post hoc* analysis with the Fisher's protected least significant difference test.

Overall differences in four miniature parameters (mEPSC/mIPSC amplitudes and

frequency) were analyzed using MANOVA with Wilks' Lambda distribution. Specific

differences between two experiences were further analyzed using *pos-hoc* MANOVAs.

Moreover, we used Mann-Whitney U test to analyze the AMPA/NMDA ratio and PPRs

of medial perforant pathway, lateral perforant pathway and mossy cells synapses of

granule cells. *P* < 0.05 was considered statistically significant.

References

Amaral, D. G., Scharfman, H. E., Lavenex, P., 2007. The dentate gyrus: fundamental neuroanatomical organization (dentate gyrus for dummies). Prog. Brain Res. 163, 3-22.

Bezaire, M. J., Soltesz, I., 2013. Quantitative assessment of CA1 local circuits: knowledge base for interneuron-pyramidal cell connectivity. Hippocampus 23, 751-785.

Bliss, T. V., Collingridge, G. L., 1993. A synaptic model of memory: long-term potentiation in the hippocampus. Nature 361, 31-39.

Bliss, T. V., Lømo, T., 1973. Long-lasting potentiation of synaptic transmission in the dentate area of the anaesthetized rabbit following stimulation of the perforant path. J. Physiol. 232, 331-356.

Bui, A. D., Nguyen, T. M., Limouse, C., Kim, H. K., Szabo, G. G., Felong, S., Maroso, M., Soltez, I., 2018. Dentate gyrus mossy cells control spontaneous convulsive seizures and spatial memory. Science 359, 787-790.

Collingridge, G. L., Kehl, S. J., McLennan, H., 1983. Excitatory amino acids in synaptic transmission in the Schaffer collateral-commissural pathway of the rat hippocampus. J. Physiol. 334, 33-46.

Danjo, T., Toyoizumi, T., Fujisawa, S., 2018. Spatial representations of self and other in the hippocampus. Science 359, 213-218. doi: 10.1126/science.aao3898.

Dolphin, A. C., Errington, M. L., Bliss, T. V. P., 1982. Long-term potentiation of the perforant path in vivo is associated with increased glutamate release. Nature 297, 496-497.

GoodSmith, D., Chen, X., Wang, C., Kim, S. H., Song, H., Burgalossi, A., Christian, K. M., Knierim, J. J., 2017. Spatial Representations of Granule Cells and Mossy Cells

of the Dentate Gyrus. Neuron 93, 677-690. doi: 10.1016/j.neuron.2016.12.026. Epub 2017 Jan 26.

Halasy, K., Somogyi, P., 1993. Distribution of GABAergic synapses and their targets in the dentate gyrus of rat: a quantitative immunoelectron microscopic analysis. J. Hirnforsch. 34, 299-308.

Hainmueller, T., Bartos, M., 2020. Dentate gyrus circuits for encoding, retrieval and discrimination of episodic memories. Nat. Rev. Neurosci. 21, 153-168. doi:10.1038/s41583-019-0260-z.

Hashimotodani, Y., Nasrallah, K., Jensen, K. R., Chavez, A. E., Carrera, D., Castillo, P. E. 2017. LTP at hilar mossy cell-dentate granule cell synapses modulates dentate gyrus output by increasing excitation/inhibition balance. Neuron 95, 928-943.

Ishikawa, J., Tomokage, T., Mitsushima, D., 2019. A possible coding for experience: ripple-like events and synaptic diversity. BioRxiv. 2019.12.30. https://doi.org/10.1101/2019.12.30.891259

Izquierdo, I., Barros, D. M., Mello e Souza, T., de Souza, M. M., Izquierdo, L. A., Medina, J. H. 1998. Mechanisms for memory types differ. Nature 393, 635-636.

Jung, M. W., McNaughton, B. L., 1993. Spatial selectivity of unit activity in the hippocampal granular layer. Hippocampus 3, 165-182. doi:10.1002/hipo.450030209.

Kida, H., Sakimoto, Y., Mitsushima, D., 2017. Slice patch clamp technique for analyzing learning-induced plasticity. J. Vis. Exp. e55876. doi:10.3791/55876.

Kida, H., Tsuda, Y., Ito, N., Yamamoto, Y., Owada, Y., Kamiya, Y., Mitsushima, D., 2016. Motor training promotes both synaptic and intrinsic plasticity of layer II/III pyramidal neurons in the primary motor cortex. Cereb. Cortex 26, 3494-3507.

Mitsushima, D., Ishihara, K., Sano, A., Kessels. H. W., Takahashi, T., 2011. Contextual

    learning requires synaptic AMPA receptor delivery in the hippocampus. Proc. Natl.

    Acad. Sci. USA. 108, 12503-12508.

Mitsushima, D., Sano, A., Takahashi, T., 2013. A cholinergic trigger drives

    learning-induced plasticity at hippocampal synapses. Nat. Commun. 4, 2760. doi:

    10.1038/ncomms3760.

Morris, R. G., Anderson, E., Lynch, G. S., Baudry, M., 1986. Selective impairment of

    learning and blockade of long-term potentiation by an N-methyl-D-aspartate

    receptor antagonist, AP5. Nature 319, 774-776.

Neuneubel, J. P., Knierim, J. J., 2014. CA3 retrieves coherent representations from

    degraded input: direct evidence for CA3 pattern completion and dentate gyrus

    pattern separation. Neuron 81, 416-427. doi: 10.1016/j.neuron.2013.11.017.

Ono, Y., Saitow, F., Konishi, S., 2016. Differential modulation of $GABA_A$ receptors

    underlies postsynaptic depolarization- and purinoceptor-mediated enhancement of

    cerebellar inhibitory transmission: a nonstationary fluctuation analysis study. PLoS

    One 11, e0150636.

Otmakhova, N. A., Otmakov N, Lisman, J. E., 2002. Pathway-specific properties of

    AMPA and NMDA mediated transmission in CA1 hippocampal pyramidal cells. J.

    Neurosci. 22, 1199-1207.

Palpagama, T. H., Sagniez, M., Kim, S., Waldvogel, H. J., Faull, R. L., Kwakowsky, A.,

    2019. $GABA_A$ receptors are well preserved in the hippocampus of aged mice.

    eNeuro 6, 1039.

Patten, A. R., Yau, S. Y., Fontaine, C. J., Meconi, A., Wortman, R. C., Christie, B. R.,

    2015. The benefits of exercise on structural and functional plasticity in the rodent

hippocampus of different disease models. Brain Plast. 1, 97-127. doi:
10.3233/BPL-150016.

Patton, P. E., McNaughton, B., 1995. Connection matrix of the hippocampal formation:
1. The dentate gyrus. Hippocampus 5, 245-286.

Pinheiro, P. S., Mulle, C., 2008. Presynaptic glutamate receptors: physiological functions
and mechanisms of action. Nat. Rev. Neurosci. 9, 423-436.

Roy, D. S., Arons, A., Mitchell, T. I., Pignatelli, M., Ryan, T. J., Tonegawa, S., 2016.
Memory retrieval by activating engram cells in mouse models of early
Alzheimer's disease. Nature 531, 508-512. doi: 10.1038/nature17172.

Sakimoto, Y., Mizuno, J., Kida, H., Kamiya, Y., Ono, Y., Mitsushima, D., 2019.
Learning promotes subfield-specific synaptic diversity in hippocampal CA1
neurons. Cereb.Cortex 29, 2183–2195. doi:10.1093/cercor/bhz022, 2019.

Scharfman, H.E., 2016. The enigmatic mossy cell of the dentate gyrus. Nature Reviews
Neuroscience 17, 562-575.

Senzai, Y., Buzsáki, G., 2017. Physiological properties and behavioral correlates of
hippocampal granule cells and mossy cells. Neuron 93, 691-704.e5. doi:
10.1016/j.neuron.2016.12.011.

Shi, S., Hayashi, Y., Esteban, J. A., Malinow, R., 2001. Subunit-specific rules governing
AMPA receptor trafficking to synapses in hippocampal pyramidal neurons. Cell
105, 331-343. doi: 10.1016/s0092-8674(01)00321-x.

Tocco, G., Maren, S., Shors, T. J., Baudry, M., Thompson, R. F., 1992. Long-term
potentiation is associated with increased [^{3}H]AMPA binding in rat hippocampus.
Brain Res. 573, 228-234.

Wang, S., 1997. Properties and interactions of the medial and lateral perforant pathways
in rat dentate gyrus. University of Toronto.

Conflict of Interests:

Acknowledgments:

Figure Legends

Figure 1. (A) Schema of the light-dark box used for the inhibitory avoidance (IA) task. (B) Thirty minutes after the brief foot-shock, the rats consistently showed a longer latency before entering the dark side of the box. (C) We then prepared brain slices after the training and analyzed synaptic currents from granule cells in the suprapyramidal area of DG. **$P < 0.01$ vs. before. Error bars indicate ± SEM. The number of rats is indicated at the bottom of each bar.

Figure 2. (A) Representative traces of mEPSCs and mIPSCs. mEPSCs at −60 mV and mIPSCs at 0 mV were measured sequentially in the same neuron in the presence of tetrodotoxin (0.5 μM). Vertical scale bar, 10 pA; horizontal scale bar, 200 ms. (B and D) Plots of mean mEPSC/mIPSC amplitudes of individual granule cells in untrained, trained, unpaired, and walk-through rats. (C and E) Plots of mean mEPSC/mIPSC frequencies of individual granule cells in the four groups. Error bars indicate ± SEM. The number of cells is indicated at the bottom of each bar. **$P < 0.01$ vs untrained.

Figure 3. (A) Post synaptic plasticity at medial perforant pathway, lateral perforant pathway and mossy cells synapses. The mean AMPA/NMDA ratios at perforant pathways and mossy cells synapses show no significance after IA task. By the combination of both MPP and LPP data, we found significant difference (a: left and middle). (B) Presynaptic plasticity at medial perforant pathway, lateral perforant pathways and mossy cells synapses. The dentate gyrus of the hippocampus where we calculated PPRs of perforant pathways and mossy cells synapses and a higher ratio suggests a lower release probability of glutamate. IA training significantly increased the PPRs at mossy cells synapses in the dentate gyrus (*).
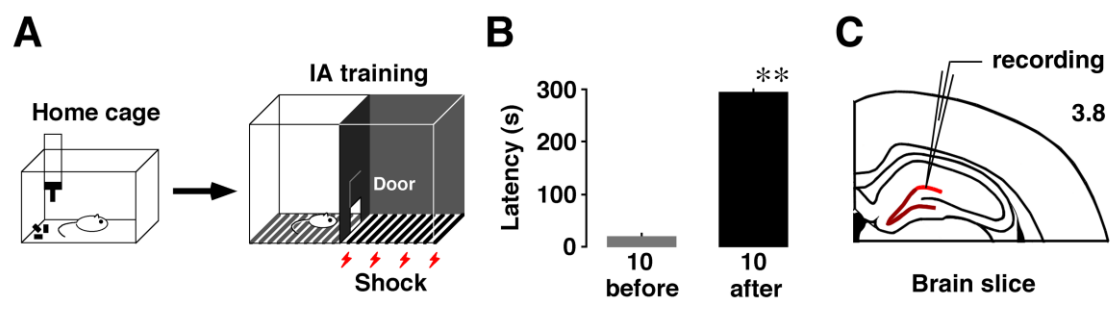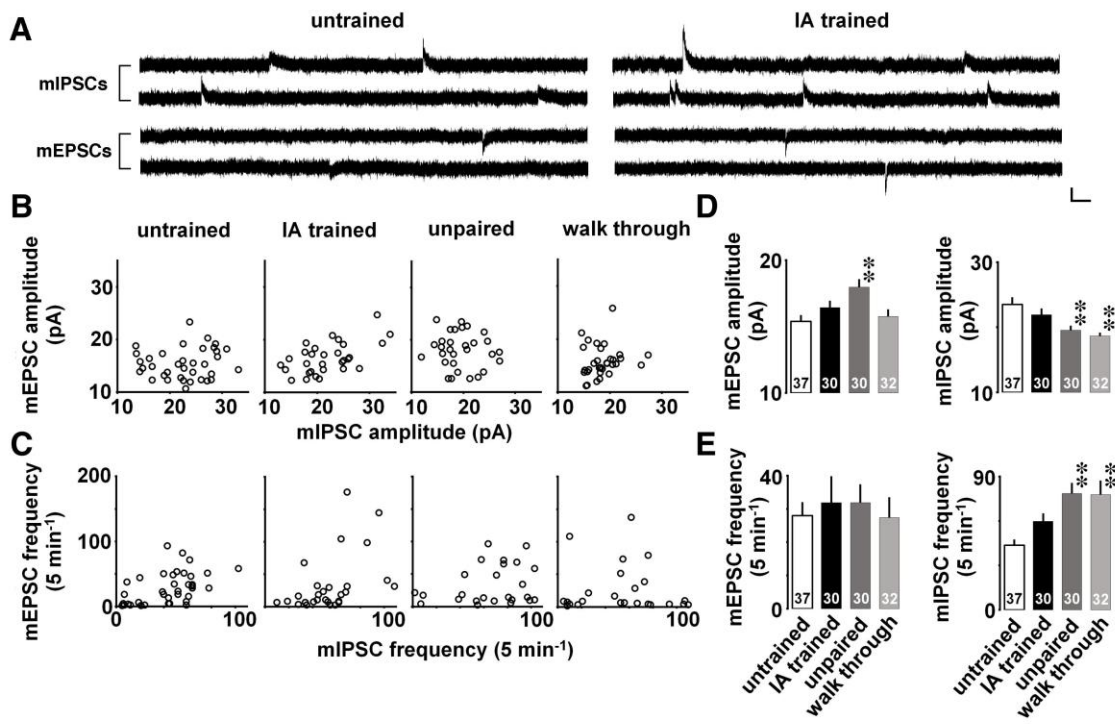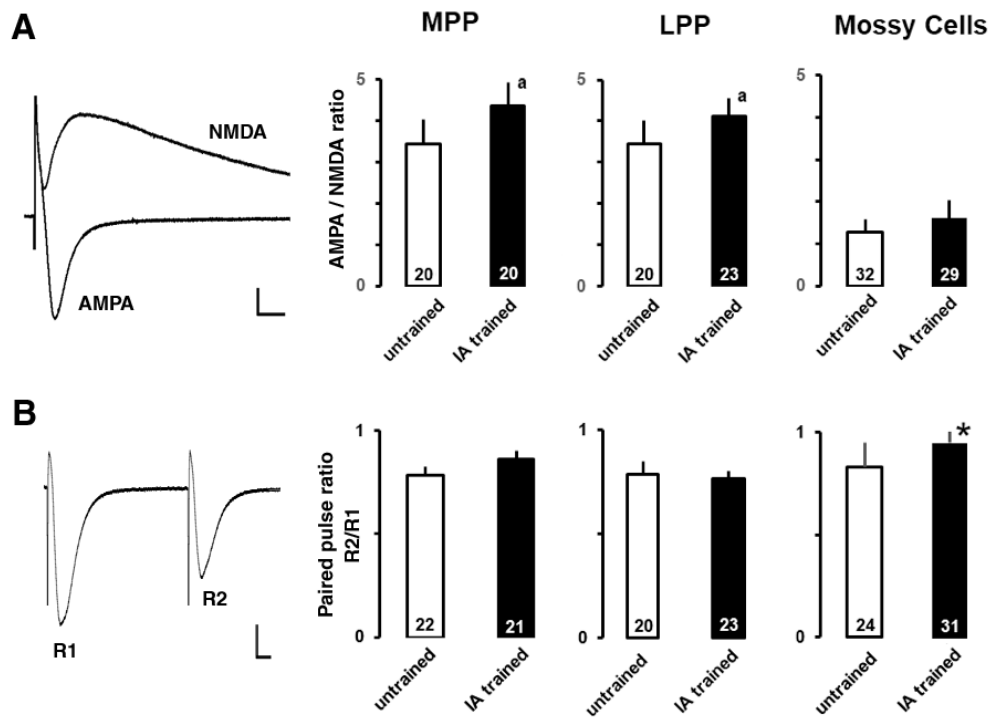
Figure 1

Figure 2

Figure 3